Study of runaway electron transport with the fractional diffusion model and comparison with experiments on COMPASS

A. Casolari[1], E. Macusova[1], J. Cerovsky[1 2], M. Farnik[1 2], O. Ficker[1 2], J. Mlynar[1], M. Gobbin[3], and the COMPASS team[1]

[1] *Institute of Plasma Physics of the CAS, Prague, Czech Republic*

[2] *FNSPE, Czech Technical University in Prague, Prague, Czech Republic*

[3] *Consorzio RFX, Padova, Italy*

Introduction

Large toroidal electric fields following a disruption event are capable of accelerating a large fraction of the electrons to relativistic energies; these energetic electrons are called "runaway electrons" (REs)[1]. REs can be trapped inside non-axisymmetric flux tubes, rapidly reforming after the thermal quench phase of the disruption [2]. RE dynamics and transport is affected by the presence of magnetic perturbations, either caused by internal MHD activity or externally generated Resonant Magnetic Perturbations (RMPs). The evidence of a coupled dynamics of REs and magnetic islands has been observed in the correlation between the Hard X Ray (HXR) signals, and the magnetic signals obtained by Mirnov pick-up coils [3]. The presence of partially broken magnetic surfaces and chains of magnetic islands makes the usual diffusive approach inadequate to the study of transport, and the fractional diffusion model should be used instead.

Experimental measurements

The magnetic perturbations present in the plasma volume can be studied by looking at the signal from Mirnov pick-up coils. By performing a phase-shift analysis on magnetic signals from aligned Mirnov coils, it is possible to calculate the poloidal mode number. The primary means of measuring RE losses at COMPASS relies on standard HXR diagnostics. The HXR radiation is mainly generated when the REs escape the plasma volume and hit the wall or the limiter, and it is directly proportional to the particle losses. The correlation between magnetic and HXR signals provides the evidence of a coupled dynamics of REs and MHD modes. In COMPASS, RE generation is favoured by a limited fuel injection in the ramp-up phase of the current, while a second gas puff causes the disruption. The RE seed formation and the losses of RE population during the flat-top phase can be be observed from HXR signal. The RE beam in the post disruption plasma is visible as a long ramp-down of the current. In this phase, the use of RMPs of different amplitude and phase proved to affect the RE suppression [4][5]. An example of COMPASS dischages with REs is displayed in Fig.1

Fractional transport and diffusion

The diffusive model is strictly valid only in the presence of completely stochastic magnetic field lines, which is the case of fully overlapping magnetic islands. This situation takes place usually just after the disruption, where the magnetic surfaces are broken. In the flat-top phase, where most of the magnetic surfaces are intact, the magnetic equilibrium can be perturbed by low-order MHD modes (magnetic islands). In general, the ordinary diffusive approach is not valid to describe the RE transport, and a fractional diffusion model should be used instead.

In the fractional diffusive regime, the mean square displacement of particle orbits grows with a fractional power of time, $\langle \Delta r^2 \rangle \sim K_\alpha t^\alpha$. Typically, the fractional exponent is below one, which means that the regime of transport is subdiffusive [6]. To account for the fractional dependence of space on time, the diffusion equation must be modified, and this can be achieved by replacing the ordinary time derivative with a fractional-order time derivative. It is possible to write a generalized diffusion equation describing the transport of REs in the presence of arbitrary magnetic configurations. In cylindrical geometry, the equation has this aspect:

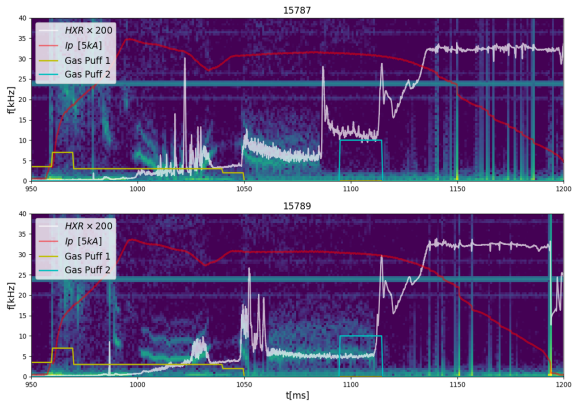

Figure 1: COMPASS discharges partially differing for the MHD ativity, which affects the RE beam evolution

$$ {}_0^C D_t^\alpha n = \frac{1}{r}\frac{\partial}{\partial r}\left(r K_\alpha \frac{\partial n}{\partial r} \right) \tag{1} $$

where ${}_0^C D_t^\alpha$ is the Caputo fractional derivative [7], which is an integral-differential operator, and K_α is a generalized diffusion coefficient, which can be defined as:

$$ K_\alpha(r,t) = Y \frac{\langle \Delta r^2 \rangle}{2(\Delta t)^\alpha} \tag{2} $$

The operation $\langle \cdot \rangle$ represents a poloidal average. Y is an energy-dependent correction that comes from the average over the finite drift orbits of the particles [8]. The average square displacement $\langle \Delta r^2 \rangle$ can be obtained by integrating the trajectories of the magnetic field lines through the Hamilton equations, which evolve the radial and poloidal position of the magnetic field lines by using the poloidal and toroidal magnetic fluxes. The time which enters Eq.2 for the diffusion coefficient can be written in terms of the toroidal angle as: $\Delta t = R\Delta\varphi / v_{||}$. The parameter α can be determined by imposing that the ratio $\langle \Delta r^2 \rangle / (\Delta t)^\alpha$ converges for large Δt.

Reconstruction of the magnetic configuration

The poloidal magnetic flux entering Hamilton equations can be reconstructed from experimental measurements. The total flux is given by an equilibrium, obtained from EFIT reconstructions [9], plus the perturbations, that can be calculated from Mirnov signals. We assume that the perturbation part consists in low-order rotating tearing modes. A general form for the total poloidal magnetic flux is $\psi = \psi_{0,0}(r) + \psi_{1,0}(r)\cos\theta + \sum_{m,n}\psi_{m,n}(r)\cos(m\theta - n\varphi + \phi_{m,n})$. The mode numbers of rotating perturbations can be obtained by performing a phase-shift analysis. The radial profile of the magnetic field perturbations can be obtained by integrating the equation for tearing eigenmodes with the appropriate boundary conditions.

Analysis of COMPASS discharges

We consider circular discharges, so that we can apply the equations and the formulas valid in cylindrical geometry, with the toroidal correction to the equilibrium. We integrated Eq.1 numerically by using a Crank-Nicolson algorithm [10]. We considered different initial density distributions n_0 for the RE beam and different values for the average RE energy. The RE density distributions we chose are shown in Fig.2. The distributions have been normalized so that the total number of particles, integrated over the volume, is the same: $N_0 = \int_0^1 n_0(r)rdr$. The time-integrated HXR signal is proportional to the total number of lost particles, that is $N_{loss} = N_0 - N(t)$. Different average RE energies can be used to find out how this affects transport. For this study, we used the energies 1MeV, 5MeV and 10MeV. We observed that, in these conditions, the energy dependent coefficient Y is approximately constant, so we chose the energy of 5 MeV.

The total particle losses for the uniform density distribution and for the chosen energy is shown in Fig.3, together with the time-integrated HXR signal. The qualitative agreement in these two shots is good, but the diffusive model fails to predict the rapid increase in the particle losses in the last 10 ms of shot 15787, which corresponds to the end of MHD activity associated with a chain of magnetic islands. This burst of HXR can be interpreted as the sudden release of a fraction of particles previously trapped inside the magnetic island.

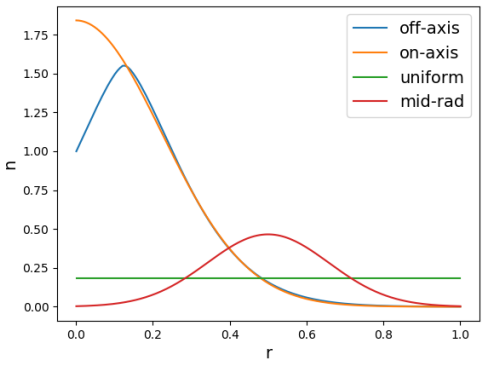

Figure 2: Initial RE density distributions

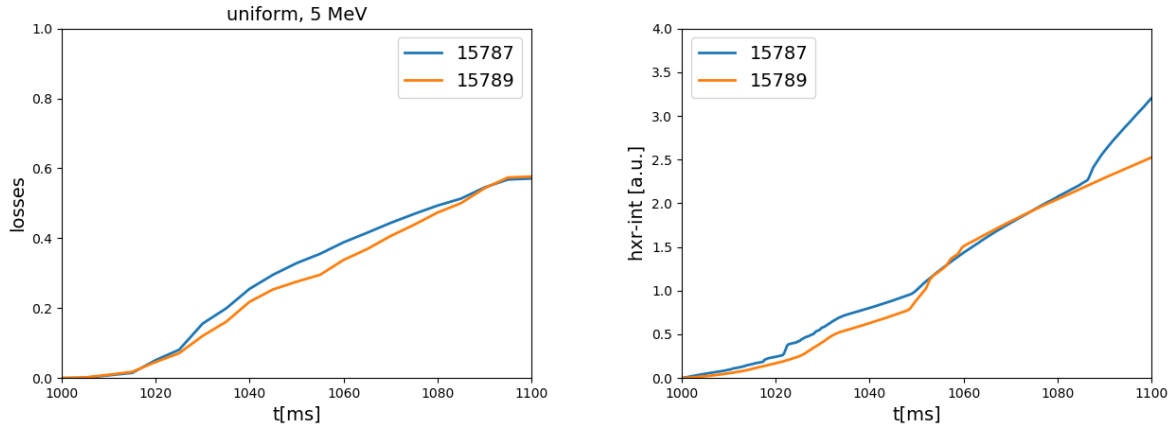

Figure 3: Numerically calculated particle losses versus time integrate HXR signal.

Conclusions

Theoretical and numerical tools for to the study of RE transport in partially stochastic magnetic fields have been developed. The comparison of the theoretical predictions for the RE density evolution with experimental measurements of HXR emission on COMPASS show some qualitative agreement. The hypotheses assumed by the model, constant RE energy and no significant RE production (avalanche), are only partially satisfied in the selected discharges. The tools that have been developed need further improvement before quantitative comparison with the experiments can be made.

Acknowledgements

This work was supported by Czech Science Foundation Project GA18-02482S and MEYS Projects 8D15001 and LM2015. The project received funding from the European Union's Horizon 2020 research and innovation programme under grant agreement No. 633053. The views and opinions expressed herein do not necessarily reflect those of the European Commission.

References

[1] H. Knoepfel et al., Nuclear Fusion **19** 785 (1979)

[2] A. H. Boozer, Physics of Plasmas **23** 082514 (2016)

[3] O. Ficker et al., Nuclear Fusion **57** 076002 (2017)

[4] M. Gobbin et al., Plasma Physics and Controlled Fusion **60** 014036 (2017)

[5] J. Mlynar et al., Plasma Physics and Controlled Fusion **61** 014010 (2018)

[6] G. Spizzo et al., Nuclear Fusion **56** 016019 (2018)

[7] M. Caputo, Geophysical Journal International **13** 529-539 (1967)

[8] T. Hauff and F. Jenko, Physics of Plasmas **16** 102308 (2009)

[9] L. C. Appel et al., 33rd EPS Conference on Plasma Physics **06** (2006)

[10] N. H. Sweilam et al., Journal of Fractional Calculus and Applications **2** 1-9 (2012)